Chapter 2. Basic Atomic Physics

Academic and Research Staff

Professor Daniel Kleppner, Professor David E. Pritchard, Professor Wolfgang Ketterle

Visiting Scientists and Research Affiliates

Dr. Theodore W. Ducas,[1] Dr. Fred L. Palmer, Dr. H. Joerg Schmiedmayer, Stefan Wehinger

Graduate Students

Michael R. Andrews, Michael P. Bradley, Michael S. Chapman, Michael W. Courtney, Kendall B. Davis, Frank DiFilippo, Joel C. DeVries, Christopher R. Ekstrom, Troy D. Hammond, Jeffrey R. Holley, Hong Jiao, Michael A. Joffe, Robert I. Lutwak, Marc O. Mewes, Vasant Natarajan, Richard A. Rubenstein, Neal W. Spellmeyer

Undergraduate Students

Ilya Entin, Philip M. Hinz, Wan Morshidi, Amrit R. Pant, J. David Pelly, Abraham D. Stroock, Bridget E. Tannian, Stanley H. Thompson, John J. Wuu, Peter S. Yesley

Technical and Support Staff

Carol A. Costa

2.1 Testing Quantum Chaos with Rydberg Atoms in Strong Fields

Sponsors

National Science Foundation
Grant PHY 89-19381
Grant PHY 92-21489
U.S. Navy - Office of Naval Research
Grant N00014-90-J-1322

Project Staff

Michael W. Courtney, Hong Jiao, Neal W. Spellmeyer, Professor Daniel Kleppner

Interest in the behavior of Rydberg atoms in strong fields has resulted in the generation of high resolution experimental spectra and accurate calculations for atoms in electric and magnetic fields and also experimental data in the low field regime for electric and magnetic fields. The principal motivation for this work has been to understand atomic systems under external perturbations similar in magnitude to the unperturbed energy. Rydberg atoms are central to this research, because field strengths available in the laboratory are comparable with atomic fields of highly-excited states. We have chosen to work with hydrogen because it is the simplest system to study. Alkali metal atoms are also of interest, because they break the zero field degeneracy of hydrogen and are much more tractable experimentally.

The quantum mechanics of alkali Rydberg atoms in strong electric fields is now believed to be well understood. Much has been learned about diamagnetic hydrogen, but some important regimes remain to be explored, and our knowledge of hydrogen needs to be extended to other alkalis. For example, we know little about the alkali Rydberg atoms in parallel electric and magnetic fields and even less about them when the fields have arbitrary or perpendicular orientation.

With the exception of hydrogen in an electric field, the classical analogues of all these systems undergo a transition from order to chaos. In seeking to understand the connection between quantum mechanics and classical chaos, the problem of hydrogen in a magnetic field has been extensively studied. However, the more general problem of Rydberg atoms in strong fields provides a richer testing ground for theories describing "quantum chaos."

We have developed techniques for carrying out high resolution laser spectroscopy on the lithium

[1] Physics Department, Wellesley College, Wellesley, Massachusetts.

atom in strong static fields. In addition, we have developed techniques for computing the spectra of alkali atoms in both strong electric and magnetic fields. The differences between lithium and hydrogen are minor for many cases of interest. In other cases, the core potential itself is the cause of classical chaos and becomes essential to consider.

In the experiment, a lithium atomic beam, excited by a laser, transfers atoms from the 2S state to the 3S state by a two-photon transition, and a second laser excites the atoms to Rydberg states.

The Rydberg atoms are detected by electric field ionization. Two methods for relating quantum spectra to the classical dynamics system are (1) periodic orbit theory and (2) use of statistical correlations. In the past year, we have made progress in testing both these methods which characterize quantum chaos.

Classically chaotic systems possess a proliferation of periodic orbits. Periodic orbit spectroscopy is a technique used to relate the quantum mechanical spectrum to the periodic orbits of the corresponding classical system.[2]

The hamiltonian of hydrogen in a magnetic field is given by

$$\mathcal{H} = \frac{p^2}{2} - \frac{1}{r} + \frac{1}{2} L_z B + \frac{1}{8} B^2 \rho^2 \qquad (1)$$

This hamiltonian can be rescaled using the relations: $r = B^{-2/3}\tilde{r}$, $p = B^{1/3}\tilde{p}$, and $L = B^{-1/3}\tilde{L}$. This gives the scaled hamiltonian,

$$\tilde{\mathcal{H}} = \frac{\tilde{\rho}^2}{2} - \frac{1}{\tilde{r}} + \frac{1}{2} \tilde{L}_z + \frac{1}{8} \tilde{\rho}^2 \qquad (2)$$

where $\tilde{\mathcal{H}} = B^{-2/3}H$. As a result, the classical dynamics depends only on the parameter $\varepsilon_B = B^{-2/3}E$ and not on E and B separately.

The semi-classical Bohr-Sommerfeld quantization condition for the two non-separable scaled coordinates $\tilde{\rho}$, $\tilde{z}$ is

$$\tilde{S} = (2\pi)^{-1} \oint (\tilde{p}_\rho d\tilde{\rho} + \tilde{p}_z d\tilde{z}) = nB^{-1/3}, \qquad (3)$$

where $\tilde{S}$ is the scaled action of a closed classical orbit. As a result, $\tilde{S} = n B^{-1/3}$ gives rise to equidistant lines on a scale $B^{-1/3}$ in a spectrum taken at constant scaled energy ε_B. In other words, each peak in the Fourier transform of a constant scaled energy spectrum corresponds to the scaled action of a periodic orbit.

This has been shown experimentally.[3] In addition, Delos and his colleagues have developed the techniques of periodic orbit theory which use classical dynamics to compute the actions of the periodic orbits and semi-classical techniques to compute the strength of the periodicities. The strength of the periodicities is called the recurrence strength, because an outgoing spherical wave will recur at times corresponding to the periods of the periodic orbits of the classical system. Figure 1 shows the Fourier transform of a computed constant scaled energy spectrum compared with the results of periodic orbit theory (courtesy of Dr. J.A. Shaw of the College of William and Mary). The recurrences from periodic orbit theory are in good agreement, except for peaks near scaled actions of 4, 8, 12, 16, and 20, which are systematically much stronger in the periodic orbit theory results. These peaks are due to the 5th, 10th, 15th, 20th, and 25th return of the orbit in the z=0 plane. These orbits have a bifurcation very close to the scaled energy shown here which makes their recurrence strength difficult to accurately compute.

We are planning periodic orbit spectroscopy both experimentally and computationally. Periodic orbit spectroscopy requires varying the energy and the magnetic field simultaneously so that scaled energy ε_B remains constant. Since our computational techniques have been verified by our experiments, and since it is easier to accurately vary E and B while maintaining a constant ε_B numerically than experimentally, we have proceeded computationally in the regions where the computations have been verified. In addition, our experiment is limited to exciting only odd-parity states of lithium. Computationally, we have been able to explore both odd and even parity hydrogen and lithium. In this way, we

---

[2] A. Holle, J. Main, G. Wiebusch, H. Rottke, and K.H. Welge, "Quasi-Landau Spectrum of the Chaotic Diamagnetic Hydrogen Atom," *Phys. Rev. Lett.* 61: 161 (1988); J.-M. Mao and J.B. Delos, "Hamiltonian Bifurcation Theory of Closed Orbits in the Diamagnetic Kepler Problem," *Phys. Rev. A* 45: 1746 (1992).

[3] A. Holle, J. Main, G. Wiebusch, H. Rottke, and K.H. Welge, "Quasi-Landau Spectrum of the Chaotic Diamagnetic Hydrogen Atom," *Phys. Rev. Lett.* 61: 161 (1988); T. van der Veldt, W. Vassen, and W. Hogervorst, "Quasi-Landau Structure of Diamagnetic Helium Rydberg Atoms," *Europhys. Lett.* 21: 9 (1993).

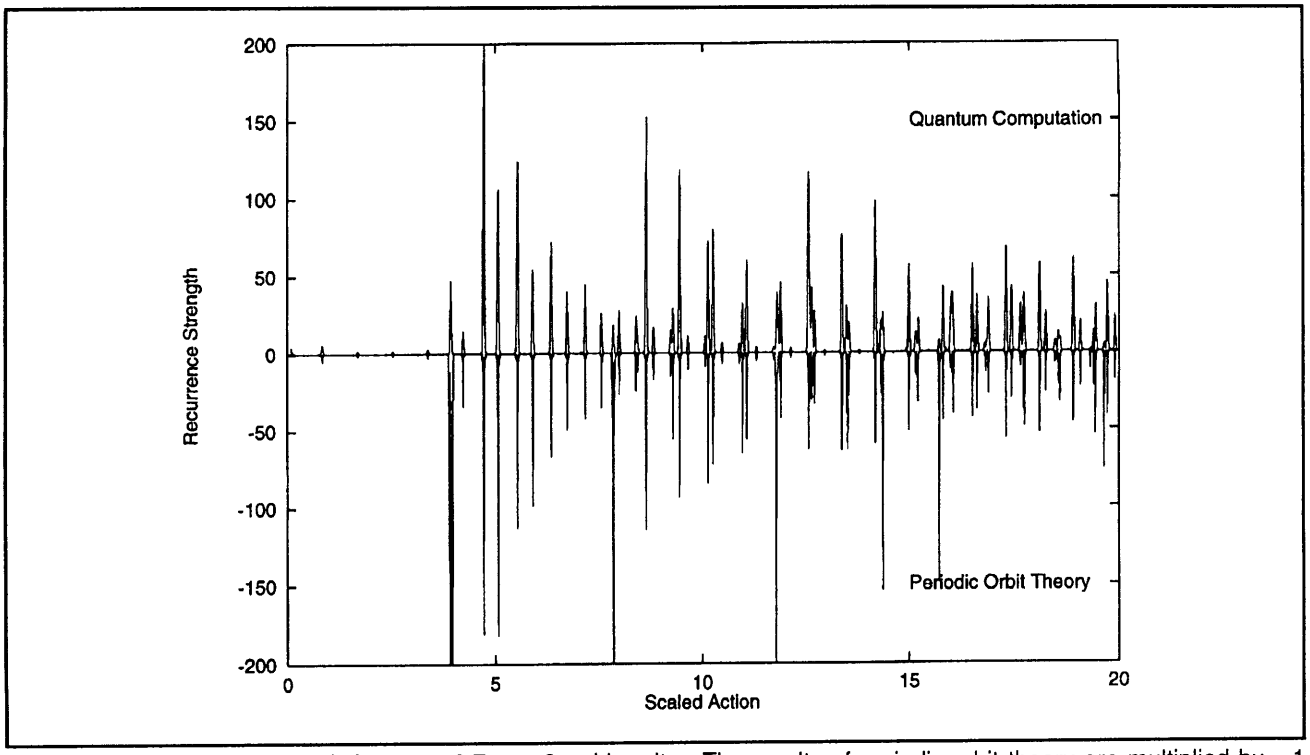

Figure 1. Recurrence strength for $\varepsilon_B = -0.7$, m = 0, odd parity. The results of periodic orbit theory are multiplied by – 1 to facilitate comparison. Each peak corresponds to a periodic orbit.

have made several discoveries with implications for periodic orbit theory.

It was previously believed that if an orbit lies on the node of the outgoing wavefunction, the recurrence strength is zero.[4] Since odd parity wavefunctions have a node in the z=0 plane, it was believed that the recurrence strength of the orbits in the z=0 plane are zero. Our quantum computations show that the recurrence strength is small but non-zero. J.A. Shaw and J.B. Delos have derived a new semiclassical formula for the recurrence strength of a periodic orbit at a node of the quantum wavefunction.[5] The results are compared with the quantum computation in figure 2.

The classical dynamics of both lithium and hydrogen in a magnetic field show a transition from order to chaos as the scaled energy is raised. However, lithium's core causes it to become chaotic at a much lower ε_B than hydrogen. As a result, lithium is completely chaotic at $\varepsilon_B = -0.6$, a value at which hydrogen is completely regular. This presents a paradox for periodic orbit theory, because it is known that the spectra of odd-parity diamagnetic lithium is nearly identical to that of hydrogen.[6] It has also been shown[7] that the energy level statistics for odd-parity lithium corresponds to a regular classical system. This is expected, since the odd parity wavefunctions have a node in the region of the chaos-causing core.

In contrast, the wavefunctions of even-parity lithium do not have a node at the core. As a result, the spectra of even-parity lithium have chaotic energy-level statistics and are very different from the spectra of even-parity hydrogen, which has regular energy level statistics. We arrive at a paradox,

---

4 M.L. Du and J.B. Delos, "Effect of Closed Classical Orbits on Quantum Spectra: Ionization of Atoms in a Magnetic Field: I and II, *Phys. Rev. A* 38: 1896-1912 (1988).

5 Private communication from Dr. J.A. Shaw, College of William and Mary, Williamsburg, Virginia.

6 C. Iu, G.R. Welch, M.M. Kash, D. Kleppner, D. Delande, and J.C. Gay, "Diamagnetic Rydberg Atom: Confrontation of Calculated and Observed Spectra," *Phys. Rev. Lett.* 66: 145 (1991).

7 G.R. Welch, M.M. Kash, C. Iu, L. Hsu, and D. Kleppner, "Experimental Study of Energy-Level Statistics in a Regime of Regular Classical Matter," *Phys. Rev. Lett.* 62: 893 (1989); G.R. Welch, M.M. Kash, C.-H. Iu, L. Hsu, and D. Kleppner, "Positive-Energy Structure of the Diamagnetic Rydberg Spectrum," *Phys. Rev. Lett.* 62: 1975 (1989).

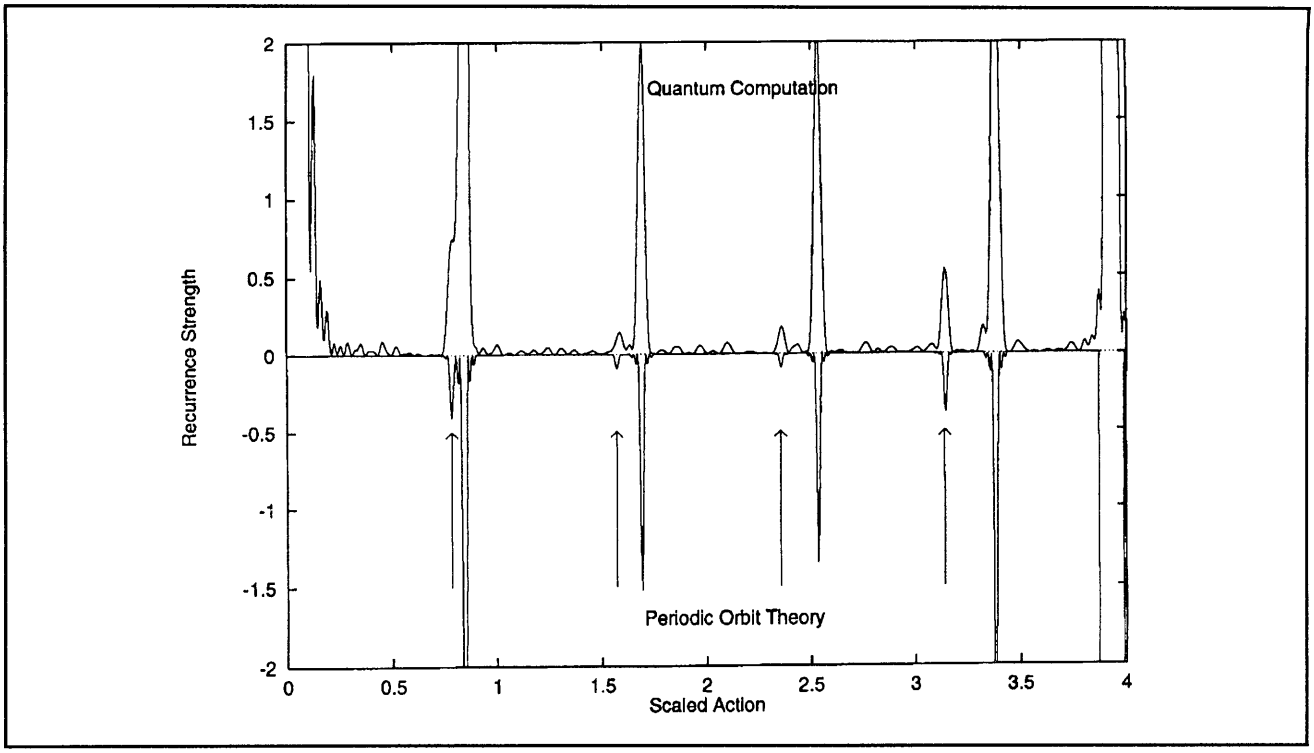

Figure 2. Recurrence strength for $\varepsilon_B = -0.7$, m = 0, odd parity. The information in figure 1 is shown enlarged 100 times. The arrows point to the orbits in the z = 0 plane.

because classical dynamics does not "know" about parity. As a result, periodic orbit spectroscopy should yield the same periodic orbits for both odd and even parity hydrogen. Similarly, periodic orbit spectroscopy in lithium should give the same periodic orbits, regardless of parity. In both hydrogen and lithium, the recurrence strengths may vary between the odd and even parity cases, because these are computed by including parity in the semiclassical methods. However, since odd parity hydrogen and lithium have nearly identical spectra, we expect the periodic orbits of lithium and hydrogen to be nearly identical. This seems to be the case from looking at the recurrences in figure 3.

However, we do not expect a completely chaotic system to have the same periodic orbits as a regular system. In addition, from a quantum mechanical point of view, we have no reason to expect that the spectrum of even parity lithium will exhibit the same periodicities as even parity hydrogen. However, figure 4 shows that many of the recurrences are the same. This is a victory for periodic orbit theory. The case of even parity lithium also has many extra recurrences, indicating extra periodic orbits. This is a challenge to periodic orbit theory, because to resolve this paradox, periodic orbit theory must find these extra periodic orbits and compute their recurrence strengths in even-parity lithium. Furthermore, it also needs to be shown that all these extra periodic orbits have a very small recurrence strength in the odd parity case.

In the case of Rydberg atoms in a strong electric field, parity is not a good quantum number. Hydrogen in an electric field is regular and chaos is caused completely by the core. The hamiltonian of hydrogen in an electric field is given by

$$\mathcal{H} = \frac{p^2}{2} - \frac{1}{r} + Fz, \tag{4}$$

and this hamiltonian can be rescaled by substituting $r = F^{-1/2}\tilde{r}$, $p = F^{1/4}\tilde{p}$. As a result, the classical dynamics of hydrogen in an electric field depends only on the parameter $\varepsilon_F = F^{-1/2}E$ and not on E and F separately. In analogy with the magnetic field case, each peak in the Fourier transform of a spectrum taken at constant ε_F corresponds to the scaled action of a periodic orbit. These classical scaling rules are exact for hydrogen and good approximations for lithium.

In the case of lithium in an electric field, we have done experiments for both the cases m = 0 and m = 1. The m = 1 case is regular and nearly identical to hydrogen, because the angular momentum barrier causes the wavefunction to have a node at the core.

The m=0 case is chaotic for all regions of interest. The experimental result for $\varepsilon_F = -0.3$ is compared with quantum computations for lithium and hydrogen in figures 5 and 6. Notice that lithium and hydrogen have many recurrences in common, but just as in the case of even-parity diamagnetic lithium, there are extra recurrences which need to be computed by periodic orbit theory. Several of these extra peaks occur near a scaled action of 14.

Spectral correlations have also been useful in characterizing spectra in regions of classical chaos. Computing the spectra in regions of total chaos has enabled the testing of a new class of universal correlations in spectra of chaotic systems as a parameter is changed. Our computations enabled MIT Professor Boris Altshuler's group to verify their new class of universal correlations on a real physical system.[8] This new class of correlations has been confirmed in the chaotic regions of both diamagnetic hydrogen and lithium.

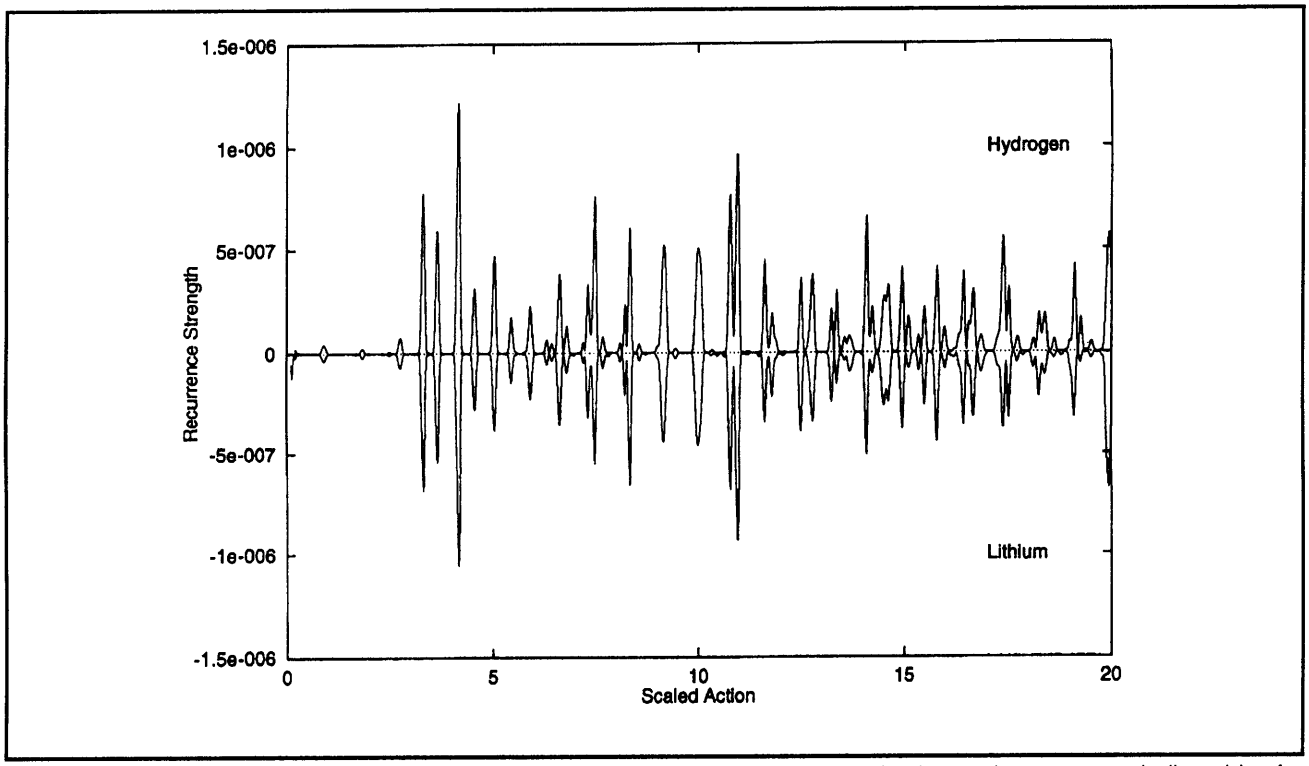

Figure 3. Recurrence strength for $\varepsilon_B = -0.6$, m = 0, odd parity. Notice that it shows the same periodic orbits for hydrogen and lithium.

[8] B.D. Simons, A. Hashimoto, M. Courtney, D. Kleppner, and B.L. Altshuler, "New Class of Universal Correlations in the Spectra of Hydrogen in a Magnetic Field," *Phys. Rev. Lett.* 71: 2899 (1993).

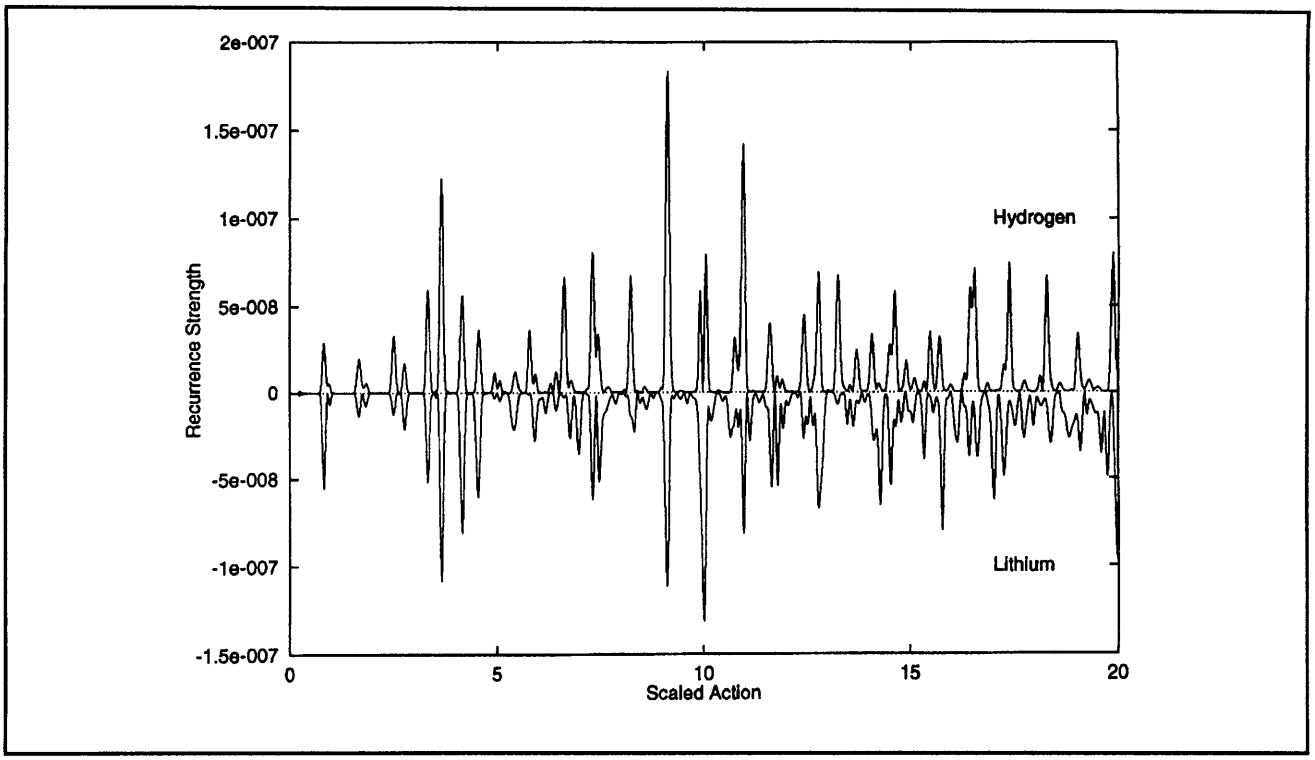

Figure 4. Recurrence strength for $\varepsilon_B = -0.6$, m = 0, even parity. Notice that it shows that lithium has many periodic orbits in common with hydrogen, but that there are extra periodic orbits present in lithium.

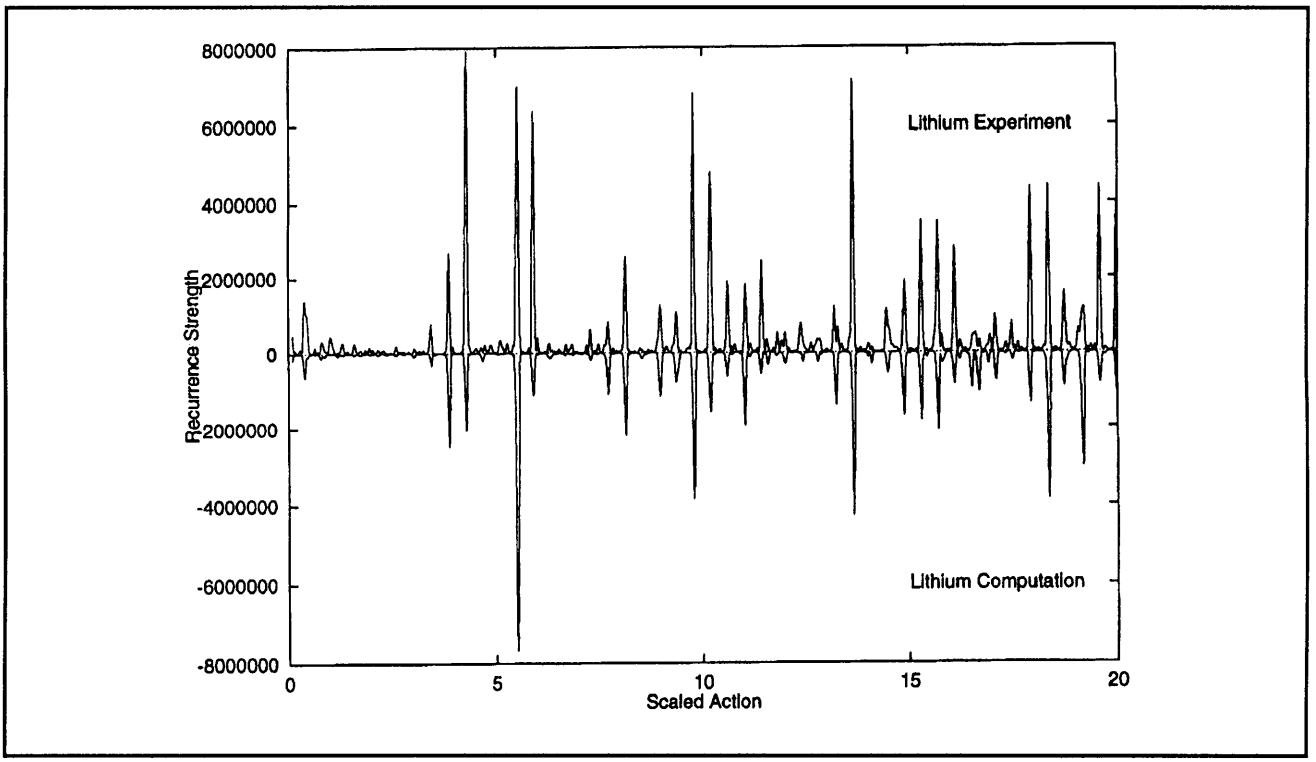

Figure 5. Recurrence strength of lithium for $\varepsilon_F = -3.0$, m = 0. The experiment is compared with quantum computations for lithium.

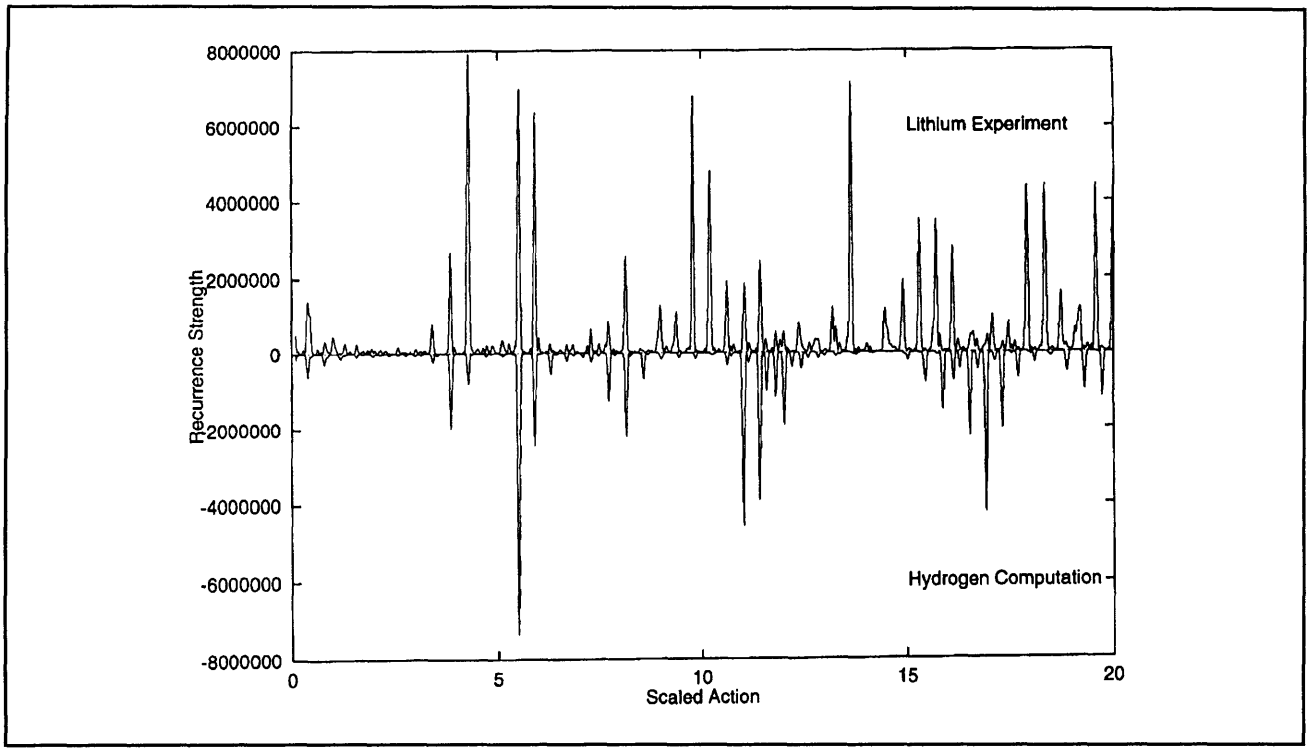

Figure 6. Recurrence strength for $\varepsilon_F = -3.0$, $m = 0$. The experiment for lithium is compared with quantum computations for hydrogen.

2.2 Millimeter-Wave Frequency Measurement of the Rydberg Constant

Sponsors

Joint Services Electronics Program
Contract DAAL03-92-C-0001
National Science Foundation
Grant PHY 89-19381
Grant PHY 92-21489

Project Staff

Joel C. DeVries, Dr. Theodore W. Ducas, Jeffrey R. Holley, Robert I. Lutwak, Professor Daniel Kleppner

The Rydberg constant R_∞ relates the wavelengths of the spectrum of atomic hydrogen to practical laboratory units. It is a so-called fundamental constant, for it relates numerous quantum properties to laboratory units. Recent advances in optical wavelength metrology have enabled experiments using laser spectroscopy to measure R_∞ with accuracy approaching two parts in 10^{11}.[9]

Although R_∞ is the most accurately measured fundamental constant, forthcoming high-precision experiments which will depend on R_∞ as an auxiliary constant, demand even more accurate measurement. Because the practical limit of measuring wavelengths, about 1 part in 10^{10}, has been reached, progress in the measurement of R_∞ requires measuring the frequency of spectral lines. Because the speed of light is now defined, by measuring cR_∞, the "Rydberg frequency," a new standard is created.

Our approach involves preparing highly excited "Rydberg" states of atomic hydrogen, n = 29, and measuring millimeter-wave transitions to nearby states. Because the millimeter wave signal is generated coherently from a frequency standard based on an atomic clock, our measurement can make use of the high precision of frequency metrology.

The goals of our experiment are three-fold: First is the reevaluation of R_∞ itself, providing an independent check, in a different regime, of other evaluations based on optical wavelength metrology. Second is the measurement of the ground state

[9] T. Andreae et al., "Absolute Frequency Measurement of the Hydrogen 1S-2S Transition and a New Value of the Rydberg Constant," *Phys. Rev. Lett.* 69: 1923 (1992); F. Nez, et al., "Precise Frequency Measurement of the 2S-8S/8D Transitions in Atomic Hydrogen: New Determination of the Rydberg Constant," *Phys. Rev. Lett.* 69: 2326 (1992).

Lamb shift. Because our measurements involve high angular momentum states for which the Lamb shift is extremely small, our results may be compared with optical measurements of transitions between low-lying states to yield an improved measurement of the Lamb shift. Third is to provide a frequency calibration of the spectrum of hydrogen, enabling the creation of a comprehensive frequency standard extending from the radio-frequency regime to the ultra-violet.

Our experiment employs an atomic beam configuration to reduce Doppler and collisional perturbations. Atomic hydrogen is excited to the low angular momentum n=29, m=0 state by two-photon stepwise absorption. The excited atoms are then transferred to the longer lived n=29, m=28 "circular" state by absorption of circularly polarized radio-frequency radiation.[10] The atoms enter a region of uniform electric field in which the frequency of the resonant transition n=29, m=28 → n=30, m=29 is measured by the method of separated oscillatory fields. The final state distribution is measured by a state-sensitive electric field ionization detector. The resonance is manifested by a transfer of atoms from the n=29 state to the n=30 state as the millimeter-wave frequency is tuned across the transition.

Figure 7 illustrates the apparatus. Atomic hydrogen or deuterium is produced by dissociating H_2 or D_2 in a radio-frequency discharge. The beam is cooled by collisions in a cryogenic thermalizing channel in order to slow the beam and thereby increase the interaction time. The atoms enter the circular state production region, where they are excited from the 1s ground state, through the 2p state, to the n=29,m=0 state by two-photon stepwise excitation. This is performed in an electric field to provide selective population of the particular n=29, m=0 level required for subsequent microwave excitation of the circular states. The electric field is then rapidly reduced to an intermediate value as the atoms pass through the center of a square configuration of four electrodes. The electrodes are excited by a 2 GHz RF source with a 90 degree phase delay between the adjacent pairs (figure 8). The circularly polarized field drives the atoms into the m=28 circular state through the stepwise absorption of 28 photons. A detector in the circular state production region monitors the efficiency of the optical excitation and angular momentum transfer processes.

After the atoms are prepared in the n=29 circular state, the beam enters the interaction region. Because Rydberg atoms interact strongly with external fields, accurate measurement of the energy level structure requires careful control of the interaction environment. Thermal radiation is reduced by cooling the interaction region to ~10K by a liquid helium flow system. The ambient magnetic field is shielded out by a double-wall high-permeablility shield. A small electric field, which defines the quantization axis of the atoms, is applied with high uniformity by field plates above

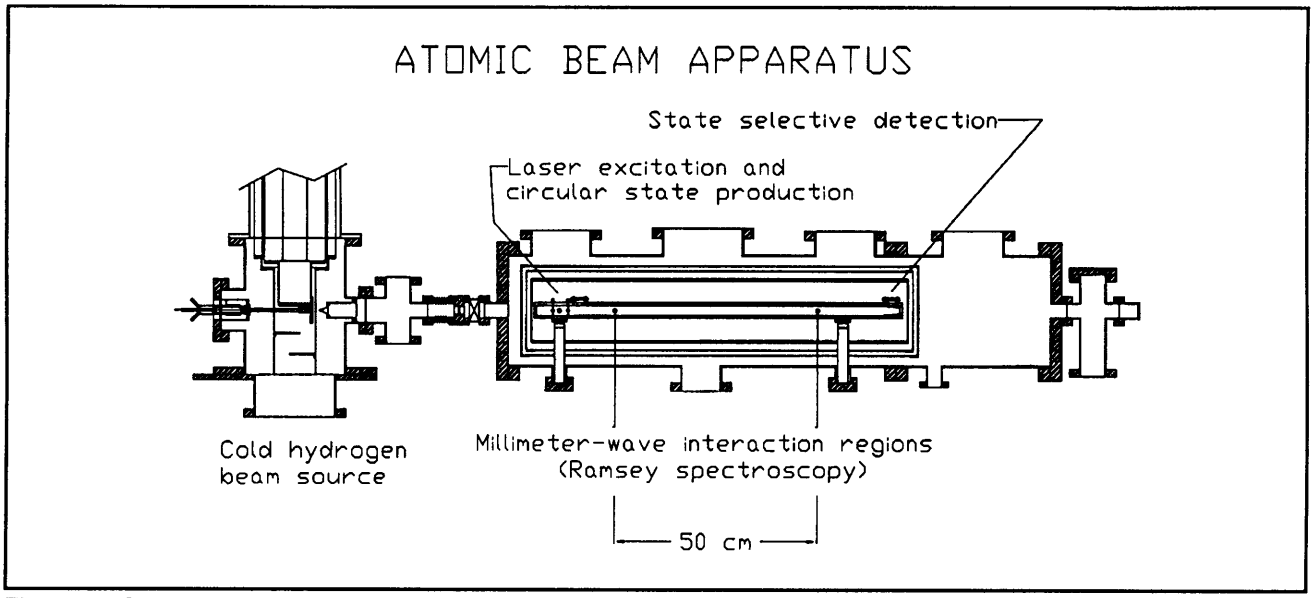

Figure 7. Schematic diagram of the atomic beam apparatus.

[10] R. Hulet and D. Kleppner, "Rydberg Atoms in 'Circular' States," *Phys. Rev. Lett.* 51: 1430 (1983).

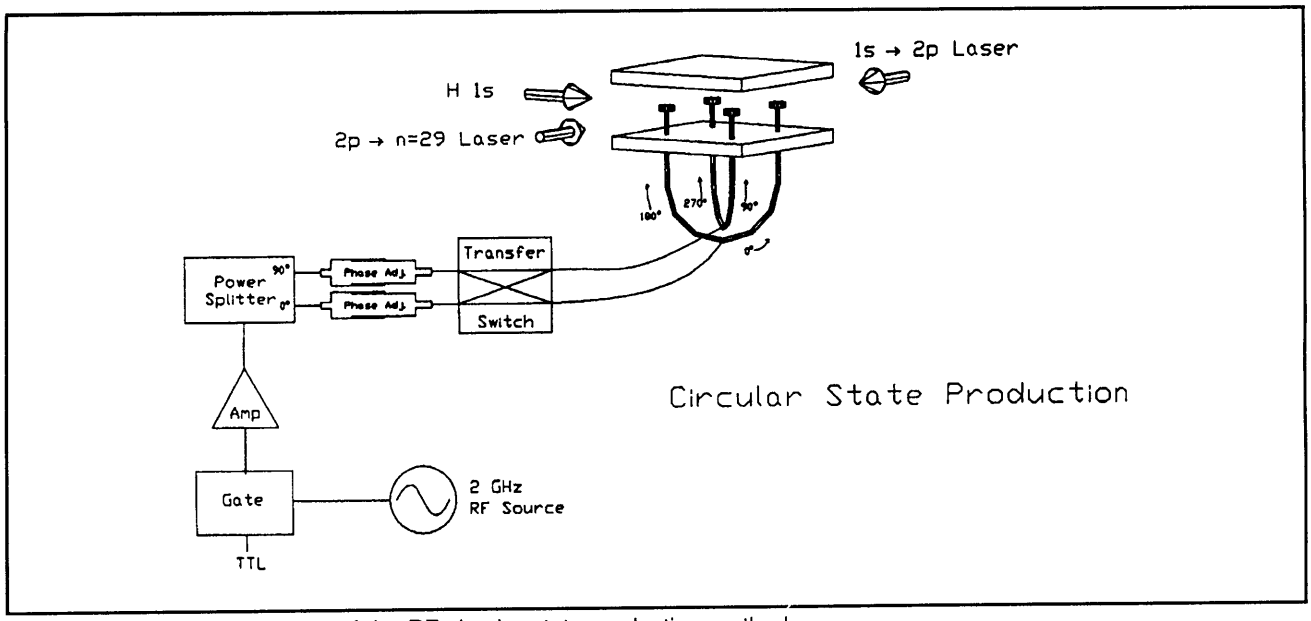

Figure 8. Schematic diagram of the RF circular state production method.

and below the atomic beam. The millimeter-waves intersect the atomic beam at two locations separated by 50 cm. The millimeter-wave optical system was described in a previous *Progress Report.*

The state distribution of the atoms emerging from the interaction region is analyzed by a state-selective electric field ionization detector. Within the detector, the atoms enter a region of increasing electric field produced by a pair of symmetric ramped plates held at constant potential. Atoms in different states are selectively ionized at different fields and the charged nuclei are detected at different positions.

We have previously presented initial data on a Ramsey interference curve. The past year was devoted to making improvements in the apparatus necessary for an accurate measurement at the level of 1 part in 10^{11}. To extract the information necessary to understand systematic sources of error, it is necessary to increase the signal-to-noise ratio of the experiment by a factor of 1000. We are accomplishing this by increasing the excitation efficiency of the atoms and decreasing the signal loss due to interaction with blackbody radiation. We have acquired an ultraviolet excimer pump laser to replace our aging YAG laser and have begun development of an ultraviolet dye laser system. This system will operate at 120 Hz instead of 10 Hz, increasing the duty cycle of the experiment from about 5 percent to 60 percent. In addition, we expect the new laser system to provide a greater spectral density and, hence, improved efficiency of atomic excitation.

On the second front, we are redesigning the atomic beam environment to reduce the temperature of the radiation fields within the interaction region. In taking preliminary data, we used the method of crossed electric and magnetic fields to transfer the atoms from the low angular momentum state to the circular state.[11] This method requires a magnetic field. Because the field could perturb the measurements, the production region had to be isolated from the interaction region. We believe that this configuration was the source of leaks of blackbody radiation into the interaction region. We have now successfully produced circular states without a magnetic field using the method of adiabatic rapid passage in a radio-frequency field (figure 9). The new atomic beam apparatus will incorporate the production, interaction, and detection of Rydberg states into one uniformly shielded region. We hope to complete the new interaction region and ultraviolet laser system in the near future, and begin performing high precision millimeter-wave spectroscopy.

[11] D. Delande and J.C. Gay, "A New Method for Producing Circular Rydberg States," *Europhys. Lett.* 5: 303 (1988).

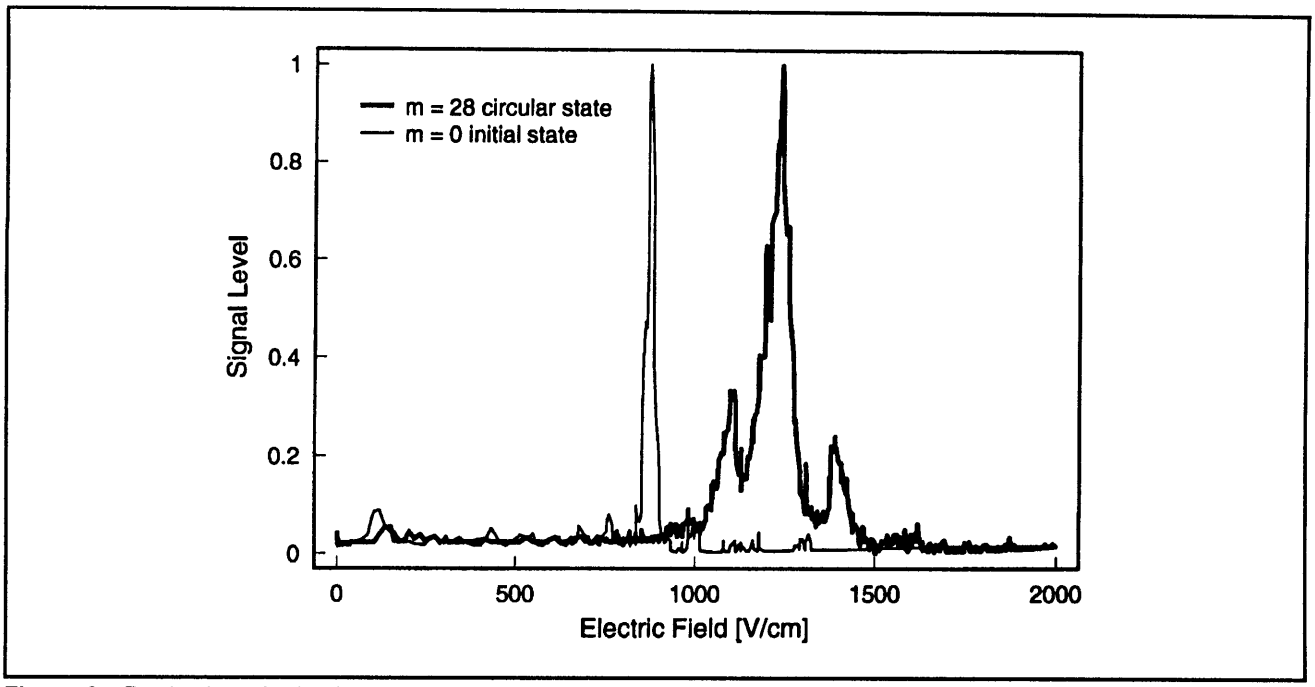

Figure 9. Production of "circular" state by absorption of circularly polarized 2 GHz radio-frequency radiation. The initial state, which ionizes at relatively low electric field (900 V/cm) appears on the left. The characteristic ionization signal of the circular state appears at roughly 1200 V/cm.

2.3 Precision Mass Spectroscopy of Ions

Sponsors

Joint Services Electronics Program
Contract DAAL03-92-C-0001
National Science Foundation
Grant PHY 89-21769

Project Staff

Michael P. Bradley, Frank DiFilippo, Vasant Natarajan, Fred L. Palmer, Abraham D. Stroock, Professor David E. Pritchard

In 1993, we developed and applied a new technique for precisely comparing the masses of two ions of widely differing atomic weight. Together with previously developed techniques, we completed a program of mass comparisons designed to determine ten atomic masses important for determination of fundamental constants or metrology. This program resulted in a new high accuracy atomic mass table with typical accuracy about 10^{-10} (an improvement of one to three orders of magnitude over previously accepted values). It also provided numerous quantitative tests of our internal consistency that virtually eliminate the possibility of unknown systematic errors. This capability has allowed us to contribute to several important experiments in both fundamental and applied physics, including:

- Contributing to a recalibration of the current x-ray wavelength standard by weighing the energy differences that go into γ-rays with wavelengths that will be measured at the National Institute of Standards and Technology;
- Determination of the molar Planck constant $N_A\hbar$, by weighing γ-rays; this will also provide an alternate determination of the fine structure constant;
- Determination of the atomic weight of ^{28}Si, which is part of a program to replace the "artifact" kilogram mass standard by a crystal of isotopically pure ^{28}Si, effectively creating an atomic standard of mass.

In addition, we are laying the groundwork for two future advances: (1) increasing the versatility of our apparatus by loading ions externally, and (2) improving our level of precision another order of magnitude. The latter goal will be achieved by comparing two simultaneously trapped ions (to eliminate the problems due to field drift) and using squeezing techniques to reduce the influence of thermal noise on the measurements. These advances will allow us to:

- Measure the $^3H^+ - {}^3He^+$ mass difference, important in ongoing experiments to determine the electron neutrino rest mass;

- Improve some traditional applications of mass spectrometry due to our orders of magnitude improvement in both accuracy and sensitivity;
- Determine the molar Planck constant $N_A\hbar$, by measuring the atomic mass and recoil velocity of an atom that has absorbed photons of known wavelength; and
- Determine excitation and binding energies of atomic and molecular ions by weighing the small decrease in mass, $\Delta m = E_{bind}/c^2$ (we must reach our ultimate goal of a precision of a few parts in 10^{-12} to make this a generally useful technique).

In our experimental approach, we measure ion cyclotron resonance on a single molecular or atomic ion in a Penning trap, a highly uniform magnetic field with confinement along the magnetic field lines provided by much weaker electric fields. We monitor the axial oscillation of the ion by detecting the currents induced in the trap electrodes. Working with only a single ion is essential because space charge from other ions leads to undesired frequency shifts. This work in trapping and precision resonance draws on techniques developed by Hans Dehmelt at the University of Washington and Norman Ramsey at Harvard, for which they shared the 1989 Nobel Prize.

We have developed techniques for driving, cooling, and measuring the frequencies of all three normal modes of Penning trap motion. Thus, we can manipulate the ion position reproducibly to within 30 microns of the center of the trap, correcting for electrostatic shifts in the cyclotron frequency to achieve greater accuracy. We use a π-pulse method to coherently swap the phase and action of the cyclotron and axial modes.[12] Therefore, although we detect only the axial motion directly, we can determine cyclotron frequency by measuring the phase accumulated in the cyclotron motion in a known time interval.

In the past two years, we have rebuilt our apparatus with a new Penning trap and quieter rf SQUID detector. We have implemented a new signal processing algorithm to improve our phase estimation by a factor of two to three. We can measure the phase of the cyclotron motion to within 10 degrees, leading to a precision of 1×10^{-10} for a one minute measurement. Our entire ion-making process has been automated, and the computer can cycle from an empty trap to having a cooled single ion in about three minutes under optimal conditions. With the spatial imperfections in the electric and magnetic fields made as small as possible our systematic errors are well below 5×10^{-11}. However, the typical statistical fluctuation in our magnetic field is 2.4×10^{-10} between measurements (over the smooth drift in the field). Thus, with the ability to achieve ~20 alternate loadings of two different ion species in one night, our overall uncertainty can be as small as 8×10^{-11} (see figure 10). We have found that the distribution of field variation is not Gaussian, but instead has additional outlying points. This has led us to use robust statistical analysis of field fluctuations; in particular, a generalization of least squares fitting called "M-estimates" in which outlying points are deweighted in a manner determined by the observed excess number of outliers. Using this analysis has eliminated arbitrary decisions about dropping "bad points" from our data sets and has increased the stability of the fit.

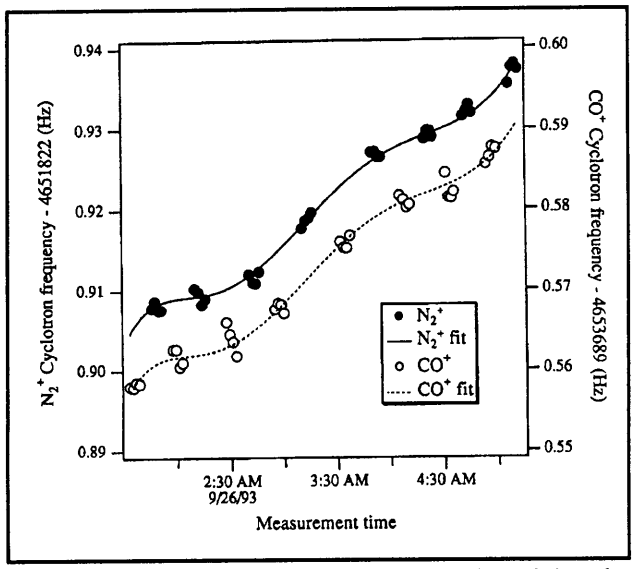

Figure 10. Cyclotron frequency as a function of time for alternate N_2^+ and CO^+ ions in our Penning trap. The frequencies are obtained after a 50s integration of cyclotron phase (see text). The solid line is a polynomial fit to the drift in the field common to both ions.

We have also developed a new measurement technique to extend our precision comparison to non-doublets (pairs of ions with substantially different mass-to-charge ratios), allowing us to perform stringent checks on systematics using such known ratios as N_2^+/N^+ and Ar^+/Ar^{++}. This technique represents a significant advance in precision mass spectrometry since it allows us to obtain absolute

[12] E.A. Cornell, R.M. Weisskoff, K.R. Boyce, and D.E. Pritchard, "Mode Coupling in a Penning Trap: π Pulses and a Classical Avoided Crossing," *Phys. Rev. A* 41: 312 (1990).

masses by direct comparison to carbon. Indeed, we have compared CD_4^+ and CD_3^+ to C^+ to obtain two independent determinations of the atomic weight of deuterium. In general, mass ratios of doublets cannot be inverted to obtain absolute masses without comparing some species to carbon, which by definition has an atomic mass of exactly 12. This is traditionally done using the ratios of very heavy ions such as $C_{13}H_{14}^+/C_{12}/H_{26}^+$ to determine H, or $C_4D_2^+/C_3D_6^+$ to determine D. We have circumvented this difficulty by developing a scheme involving only doublet comparisons that uses the known Ar^+/Ar^{++} ratio to obtain the absolute masses of several light atoms—H, D, N, O, Ne, Ar—to about an order of magnitude better than the current standard mass table (see table 1). The value of the deuterium mass obtained using this method is consistent with the value from the direct non-doublet comparisons, giving us high confidence in our results.

An extensive series of quantitative systematic checks of our results involving repeated checks of identical ratios (some interspaced by a significant reduction of our field inhomogeneities); checks of circular ratios (e.g., A/B, B/C, and C/A); checks of related ratios (e.g., CO/N_2 and CO_2/N_2O); and known ratios (e.g., Ar^{++}/Ar^+) has shown us that there are no unknown systematic errors in our results. H and D have been measured by several independent routes, because the mass of many interesting ions can be determined by comparison with a suitable organic compound of the same nominal mass.

To extend the applicability of our current mass measurement capabilities, we have built an external ion source and associated optics that can produce and select ions with a resolution of 0.1 in mass-to-charge ratio. When this comes on line, we should be able to greatly reduce the percentage of "bad" ions (wrong nominal atomic weight) and also alleviate the problem of residual neutral gas when using volatile species such as helium.

In order to proceed to much higher levels of mass measurement precision, we must eliminate the random fluctuations of the magnetic field in our measurements. We have explored two ways to achieve this by putting two ions in the trap at the same time and have decided to pursue a method

Atom	Mass (amu)	Accepted values (amu)
^1H	1.007 825 031 6 (5)	1.007 825 035 0 (120)
n	1.008 664 923 5 (23)	1.008 664 919 0 (140)
^2H	2.014 101 777 9 (5)	2.014 101 779 0 (240)
^{13}C	13.003 354 838 1 (10)	13.003 354 826 0 (170)
^{14}N	14.003 074 004 0 (12)	14.003 074 002 0 (260)
^{15}N	15.000 108 897 7 (11)	15.000 108 970 0 (400)
^{16}O	15.994 914 619 5 (21)	15.994 914 630 0 (500)
^{20}Ne	19.992 440 175 4 (23)	19.992 435 600 0 (22000)
^{28}Si	27.976 926 532 4 (20)	27.976 927 100 0 (7000)
^{40}Ar	39.962 383 122 0 (33)	39.962 383 700 0 (14000)

Table 1. Atomic mass table. The center column lists the atomic masses determined from our experiment, and the right column lists the accepted atomic masses from the 1983 evaluation. [A.H. Wapstra and G. Audi, "The 1983 Atomic Mass Evaluation (I). Atomic Mass Table," *Nucl. Phys. A* 432:1 (1985).] For the purpose of comparison, zeros have been added to the numbers in the right column so that the number of digits are equal.

we described last year.[13] If this works well, the primary source of measurement noise will be the special relativistic mass shift due to thermal fluctuations in cyclotron amplitude.

We have proposed a scheme of classical squeezing with parametric drives to reduce amplitude fluctuations.[14] In 1993, we were successful in demonstrating a simplified version of the quadrature squeezing of the thermal motion of the ion. Figure 11 shows how the rms fluctuations of the cyclotron amplitude vary when we apply a cyclotron pulse of adjustable phase to a previously squeezed distribution. Note that at θ = 90 degrees, the fluctuations are reduced to approximately one half of their unsqueezed value.[15]

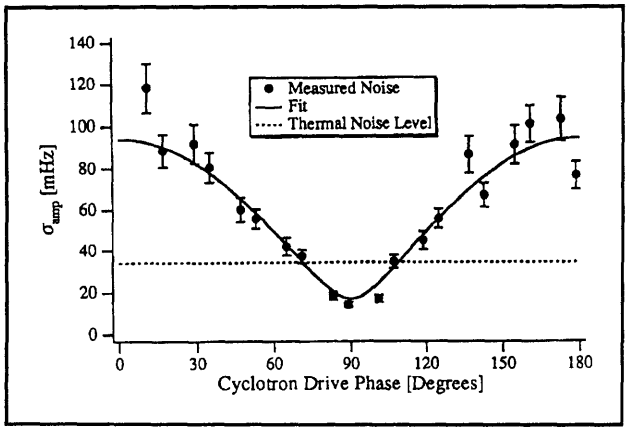

Figure 11. Demonstration of classical amplitude squeezing. The observed amplitude noise is plotted as a function of the relative phase. At a drive phase of 90 degrees, the noise is minimized. A best fit to the data shows that a factor of two reduction has been achieved.

Thesis

Natarajan, V. *Penning Trap Mass Spectroscopy at 0.1 ppb.* Ph.D. diss., Dept. of Physics, MIT, 1993.

2.4 Atom Interferometry

Sponsors

Joint Services Electronics Program
Contract DAAL03-92-C-0001
U.S. Army - Office of Scientific Research
Grant DAAL03-92-G-0229
U.S. Navy - Office of Naval Research
Grant N00014-89-J-1207

Project Staff

Michael S. Chapman, Christopher R. Ekstrom, Troy D. Hammond, Amrit R. Pant, Richard A. Rubenstein, Dr. H. Joerg Schmiedmayer, Bridget E. Tannian, Stefan Wehinger, Professor David E. Pritchard

During 1993, we refined our atom interferometer[16] and started to perform experiments with spatially separated beams. The interferometer is now operating with smaller period gratings,[17] providing greater beam separation. The experiments were performed with the aid of an interaction region that inserts a thin metal foil between the beams (figure 12). This allowed us to manipulate the atomic wave function in one arm of the interferometer without affecting the other portion.

---

[13] E.A. Cornell, K.R. Boyce, D.L.K. Fygenson, and D.E. Pritchard, "Two Ions in a Penning Trap: Implications for Precision Mass Spectroscopy," *Phys. Rev. A* 45: 3049 (1992).

[14] F. DiFilippo, V. Natarajan, K.R. Boyce, and D.E. Pritchard, "Classical Amplitude Squeezing for Precision Measurements," *Phys. Rev. Lett.* 68: 2859 (1992).

[15] F. DiFilippo, *Precise Atomic Masses for Determining Fundamental Constants*, Ph.D. diss., Dept. of Physics, MIT, 1994.

[16] D.W. Keith, C.R. Ekstrom, Q.A. Turchette, and D.E. Pritchard, "An Interferometer for Atoms," *Phys. Rev. Lett.* 66: 2693 (1991).

[17] D.W. Keith, M. Rooks, C.R. Ekstrom, D.W. Keith, and D.E. Pritchard, "Atom Optics Using Microfabricated Structures," *Appl. Phys. B* 54: 369 (1992).

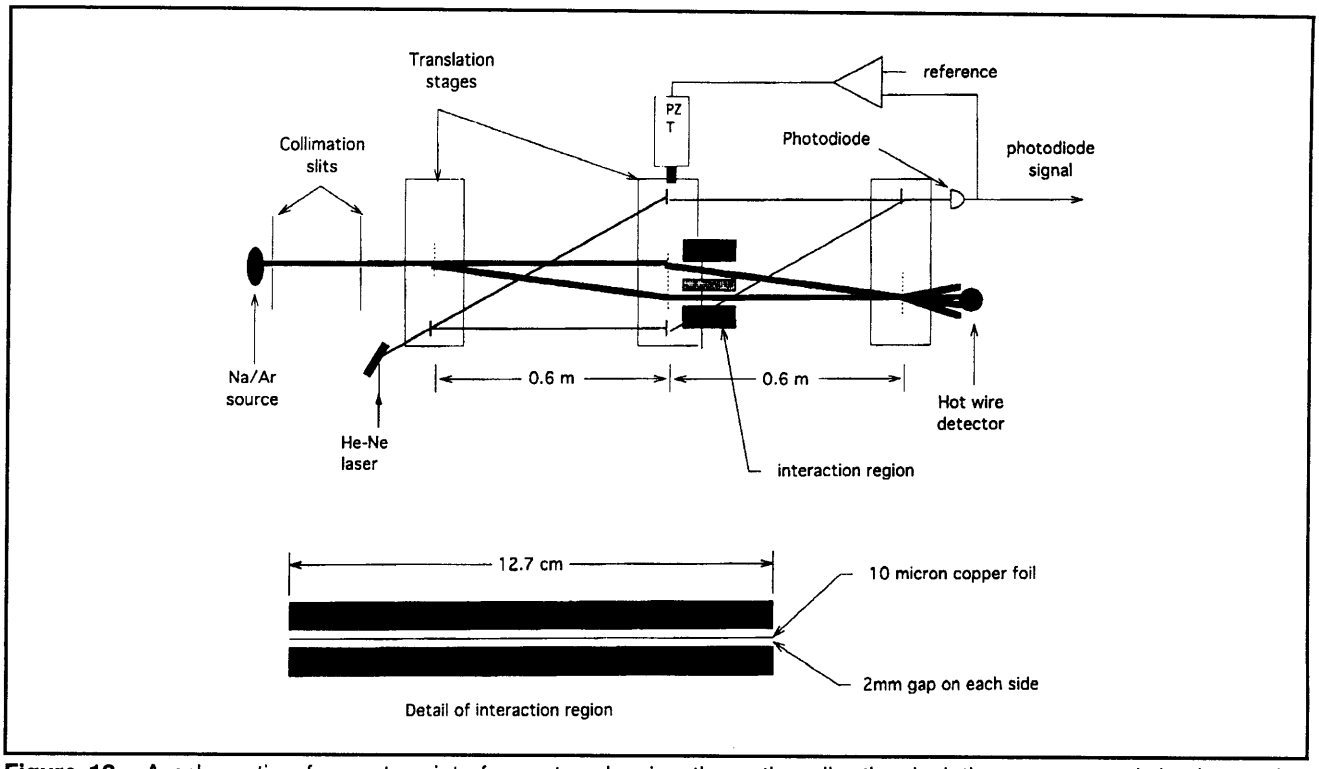

Figure 12. A schematic of our atom interferometer showing the active vibration isolation system and the interaction region (not to scale). The 10 μm copper foil is shown between the two arms of the interferometer (thick lines are atom beams). The optical interferometer (thin lines are He-Ne beams) is used for active vibration isolation. The 200 nm period atom gratings are indicated by a vertical dashed line, and the 3.3 μm period optical gratings by a vertical solid line.

Approximately six atom interferometers have been demonstrated since our pioneering demonstration of an interferometer[16] made with three nanofabricated atom gratings.[17] These instruments will make possible new types of experiments involving inertial effects, novel studies of atomic and molecular properties, and tests of fundamental physics. They could also make possible the development of ultrasmall structures using atom lithography. Specifically:

- The relatively large mass and low velocity of atoms makes atom interferometers especially sensitive to inertial effects such as rotation, acceleration, and gravity. Sagnac rotation has been observed in accord with theoretical predictions[18] and sensitivity to gravitational acceleration at the 3×10^{-8} level has been demonstrated.[19] Atom interferometers may become the best absolute accelerometers and gravimeters within the next few years.
- Atom interferometers can be applied to a number of experiments in fundamental physics: tests of quantum mechanics such as the Aharonov-Casher effect;[20] geometric phases and the measurement process; measurement of the equality of proton and electron charges; and a precise measurement of the momentum of a photon. This latter measurement should produce a new high precision value for the molar Planck constant $N_A\hbar$.
- Interferometers for atoms and molecules will provide more accurate ways to measure intrinsic properties of these particles, like their polarizability. They will also open up new areas of study, such as measurements of the "index

[18] F. Riehle, T. Kisters, A. Witte, J. Helmcke, and C.J. Borde, "Optical Ramsey Spectroscopy in a Rotating Frame: Sagnac Effect Matter-Wave Interferometer," *Phys. Rev. Lett.* 67: 177 (1991).

[19] M. Kasevich and S. Chu, "Atomic Interferometry Using Stimulated Raman Transitions," *Phys. Rev. Lett.* 67: 181 (1991).

[20] Y. Aharonov and A. Casher, "Topological Quantum Effects for Neutral Particles," *Phys. Rev. Lett.* 53: 319 (1984).

of refraction" of a gas for a propagating particle beam.

The key component of our interferometer is the set of three matched transmission diffraction gratings with 2000 Å period which we constructed at the National Nanofabrication Facility (NNF) at Cornell University. The process that we developed allows fabrication of precisely positioned openings in thin silicon nitride membranes mounted in silicon frames. Grating patterns in the membranes are generated by electron beam lithography, making the process quite versatile. This process was used to create a variety of diffraction gratings used in the interferometer. In addition, several zone plates (atom lenses) were also built and demonstrated.[21]

During 1993, we made several modifications to our atom interferometer, including the addition of a new computer interface that allows a MacIntosh Quadra with Labview software to control the experiment and analyze the data in real time. These have resulted in larger signals and greater reliability for this instrument, which is the only atom interferometer in which interfering beams are physically separated. We have exploited this capability to perform several unique experiments.

We have used this interferometer to determine the polarizability of the ground state of sodium to 0.3 percent by applying a uniform electric field to one component of the atom wave and measuring the resulting phase shift of the interference pattern. This type of measurement determines the ground state polarizabilities rather than the difference of ground and excited state polarizability which can be measured with spectroscopic or interferometric techniques in which the interfering paths are not spatially isolated. The precision of our measurement was about five times better than previous determinations.[22]

In another experiment, performed with a new interaction region that can confine a gas sample so that only one of the atom beams in the interferometer passes through it, we observed both the attenuation and the phase shift of an atomic sodium matter wave when it was transmitted through a number of atomic (He, Ne, Ar, Kr, Xe) and molecular gases (N_2, CO_2, NH_3, and H_2O). From the perspective of wave optics, the passage of a wave through a medium is described in terms of a complex index of refraction where N is the density of the medium and is the scattering amplitude. The phase shift (attenuation) is proportional to the real (imaginary) part of the forward scattering amplitude, allowing us to determine both of these quantities.[23]

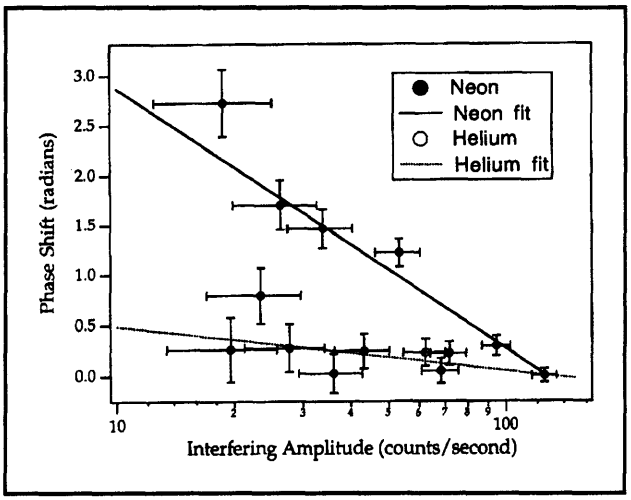

Figure 13. Phase shift versus the amplitude of the interference fringes for helium and neon. The slope of the fit on a semi-log plot as shown here is minus the ratio of the real to imaginary parts of the forward scattering amplitude.

This is the first time that the real part of the forward scattering amplitude has been measured for atom-atom scattering. An indication of the relative sensitivity of the real part to the interatomic potential is that this quantity varies over more than an order of magnitude in the systems studied. In contrast, the imaginary part of the forward scattering amplitude, which is proportional to the total scattering cross section, varies by about a factor of less than two. We therefore considered several simple models that predict the ratio of real to imaginary parts of the forward scattering amplitude for atom-atom scattering in order to elucidate the basic physics of this quantity. All of these models are based on the partial wave expression for scattering by a central potential, a treatment appropriate for our situation where the wavelength of the scattered wave is much smaller than the size of this potential.

If the collision is modeled as a hard sphere, the partial wave scattering phase shifts are nearly

---

[21] D.W. Keith, M. Rooks, C.R. Ekstrom, D.W. Keith, and D.E. Pritchard, "Atom Optics Using Microfabricated Structures," *Appl. Phys. B* 54: 369 (1992).

[22] C.R. Ekstrom, J. Schmiedmayer, M.S. Chapman, T.D. Hammond, and D.E. Pritchard, "Measurement of the Electric Polarizability of Sodium with an Atom Interferometer," submitted to *Phys. Rev. Lett.*

[23] C.R. Ekstrom, *Experiments with a Separated Beam Atom Interferometer*, Ph.D. diss., Dept. of Physics, MIT, 1993.

random, and the ratio of the real to imaginary parts of the forward scattering amplitude is predicted to be about 0.01 for He, not too far from the measured value (0.1). A van der Waals potential should produce a ratio of 0.73, in rough accord with the rare gas atoms with the largest polarizability, Xe(0.7) and Kr(0.6). Understanding the results for Ne(1.0) and Ar(0.5) will require fuller treatment, based on more realistic interatomic potentials.

Recently, we have changed the velocity of the sodium in our interferometer by changing the mass of the carrier gas in our seeded supersonic oven. This has enabled us to measure the dispersion of the index of refraction (i.e., its dependence on deBroglie wavelength) over a factor of two in wavelength.

We have also applied our atom optics techniques to molecules. Molecules were produced by optimizing the operating parameters of our seeded supersonic source so that sodium dimers constituted 30 precent of the detected beam intensity. The atoms were then removed from the beam by deflecting them with resonant laser light which was frequency stabilized to our atomic beam. Figure 14 shows diffraction of molecules and atoms and diffraction of only molecules from a 100 nm period diffraction grating.

We have used this molecular beam in our separated beams interferometer, measuring the ratio of real and imaginary parts of the forward scattering amplitude for collisions of these dimers with He and Ne. The results are the same within experimental error as for atomic sodium.

Lastly, we have demonstrated the Talbot effect, the self-imaging of a periodic structure, with atom waves. We have measured the successive recurrence of these self-images as a function of the distance from the imaged grating. This is a near field interference effect that has several possible applications in the rapidly growing field of atom lithography.

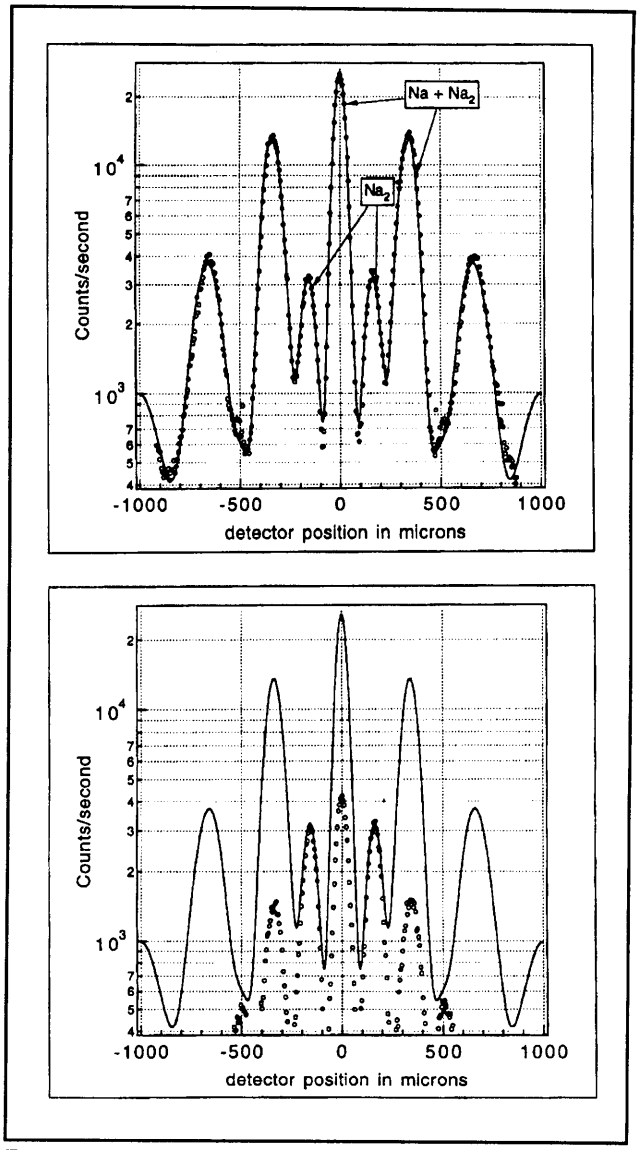

Figure 14. The top graph shows diffraction of sodium atoms and sodium dimers by a 100 nm period diffraction grating. The fit indicates 16.5 precent of the intensity is molecules, which have half the diffraction angle of the sodium atoms. The bottom graph shows the diffraction pattern after the atoms have been removed from the beam with a deflecting laser beam. The fit is the same as in the top graph, indicating that the small orders in the top graph were entirely molecules.

2.4.1 Publications

Ekstrom, C.R., J. Schmiedmayer, M.S. Chapman, T.D. Hammond, and D.E. Pritchard. "Measurement of the Electric Polarability of Sodium with an Atom Interferometer." Submitted to *Phys. Rev. Lett.*

Ekstrom, C.R., D.W. Keith, and D.E. Pritchard. "Atom Optics Using Microfabricated Structures." *App. Phys. B* 54: 369 (1992).

Pritchard, D.E. "Atom Interferometers." *Proceedings of the 13th International Conference on Atomic Physics,* Munich, Germany, August 3-7, 1992. Eds. T.W. Hansch and H. Walther. Forthcoming.

Pritchard, D.E., C.R. Ekstrom, J. Schmiedmayer, M.S. Chapman, and T.D. Hammond. "Atom Interferometry." *Proceedings of the Eleventh International Conference on Laser Spectroscopy,* June 13-18, 1993. Eds. L.A. Bloomfield, T.F. Gallagher, and D.J. Larson. New York:

American Institute of Physics, 1993. Forthcoming.

Pritchard, D.E., T.D. Hammond, J. Schmiedmayer, C.R. Ekstrom, and M.S. Chapman. "Atom Interferometry." *Proceedings of the Conference Quantum Interferometry,* Trieste, Italy, March 2-5, 1993. Eds. F. DeMartini, A. Zeilinger, and G. Denardo. Singapore: World Scientific, 1993. Forthcoming.

Schmiedmayer, J., C.R. Ekstrom, M.S. Chapman, T.D. Hammond, and D.E. Pritchard. "Atom Interferometry." *Proceedings of the Seminar on Fundamentals of Quantum Optics III,* Kuhtai, Austria, 1993. Forthcoming.

Turchette, Q.A., D.E. Pritchard, and D.W. Keith. "Numerical Model of a Multiple Grating Interferometer." *J. Opt. Soc. Am. B* 9: 1601 (1992).

Thesis

Ekstrom, C.R. *Experiments with a Separated Beam Atom Interferometer.* Ph.D. diss., Dept. of Physics, MIT, 1993.

2.5 Cooling and Trapping Neutral Atoms

Sponsors

Joint Services Electronics Program
Contract DAAL03-92-C-0001
U.S. Navy - Office of Naval Research
Grant N00014-90-J-1642

Project Staff

Michael R. Andrews, Kendall B. Davis, Ilya Entin, Philip M. Hinz, Michael A. Joffe, Marc O. Mewes, Wan Morshidi, J. David Pelly, Stanley H. Thompson, John J. Wuu, Peter S. Yesley, Professor Wolfgang Ketterle, Professor David E. Pritchard

Our current objective is to obtain samples of atoms at very high density and ultra-low temperatures. This goal is pursued by using a high flux slower for atoms, a light trap to stop and compress the atoms, and a magnetic trap for the final confinement and cooling.

Experiments with dense samples of cold neutral atoms promise exciting new discoveries in basic and applied physics. Due to the considerably reduced thermal motion of atoms, they are ideal for high resolution spectroscopy and for more accurate atomic frequency standards. In addition,

- Collisions of ultra-cold atoms in such samples are characterized by a long deBroglie wavelength and are dominated by weak long-range interactions. Since the collision duration for slow atoms greatly exceeds the radiative decay time, stimulated and spontaneous radiative transitions can take place during the collision. Slow collisions are therefore fundamentally different from fast collisions studied so far and are becoming an exciting new field of atomic physics.[24]
- High density samples of atoms open possibilities for observing quantum collective effects such as Bose-Einstein condensation and collectively enhanced or suppressed radiative decay.

In 1993, we completed the work on a dark light trap which enabled us to confine more than 10^{10} atoms at densities one to two orders of magnitude higher than achieved before. The key feature of the dark trap is that the atoms spend most of their time in a dark hyperfine state which does not scatter the trapping light.[25]

The main focus of our work has been to obtain high densities and long trapping times in a magnetic trap which was loaded from the dark light trap. The product of density and trapping time is the crucial parameter for achieving evaporative cooling.

2.5.1 Magnetic Trapping of Sodium Atoms

We have captured up to 10^{11} atoms in a dark light trap and transferred them into a magnetic trap. By counting the number of atoms before and after the transfer, we determined the transfer efficiency to be 25 percent—in coarse agreement with the 33 percent expected for trapping one out of three equally populated F=1 hyperfine states. The transfer was accomplished in a "mode-matched"

---

[24] Symposium on Cold Atom Collisions, Institute for Theoretical Atomic and Molecular Physics at the Harvard-Smithsonian Center for Astrophysics, Cambridge, Massachusetts, April 26-28, 1992, Extended Abstracts.

[25] W. Ketterle, K.B. Davis, M.A. Joffe, A. Martin, and D.E. Pritchard. "High Densities of Cold Atoms in a Dark Spontaneous-force Optical Trap." *Phys. Rev. Lett.* 70: 2253-2256 (1993).

way—both confinement volume and temperature were preserved by carefully adjusting the strength of the magnetic trapping field. Atomic densities in the magnetic trap were 10^{11} cm^{-3}.

Long trapping times were achieved by considerably improving the vacuum. Optimized differential pumping between the oven and trapping chambers allows pressure ratios of 1000. Ultimate pressures are below 10^{-10} Torr, even with the intense atomic beam on, resulting in trapping times approaching one minute. Trapping times in the light trap are longer by roughly a factor of five because of larger trap depth.

2.5.2 Dark Molasses

The temperature of atoms captured in a spontaneous light force trap can be further reduced by applying a cooling scheme called polarization-gradient molasses after switching off the magnetic field. Until now, one has encountered increased ultimate temperatures for the highest densities of atoms.[26]

We are currently investigating the idea that these high density effects can be avoided by using a dark version of molasses where most of the atoms are optically pumped into a dark hyperfine state, with only a small fraction of them in the optically cooled hyperfine state. This process ensures transparency of the atom cloud for the cooling light despite very high column densities. So far, we have successfully cooled samples to 60 μK. This temperature is below the Doppler limit of 240 μK, but higher than temperatures observed for Na at very low atomic densities (20 μK) using polarization gradient molasses.[27] We are currently studying the limits in the ultimate temperature of dark molasses. Our atom clouds have optical densities of 200 for resonant repumping light and would be opaque for the cooling light without optical pumping into a dark state.

2.5.3 Rf Induced Evaporative Cooling of Atoms

We hope to reach the nK regime using evaporative cooling instead of optical cooling. Evaporative cooling of atomic hydrogen below the recoil limit has been achieved by Professors Kleppner and Greytak,[28] but their method is highly specialized and limited exclusively to hydrogen. We believe that it is important to pursue similar goals with other atoms, not only because different atomic species such as the alkalis will show different physical effects, but also because of their ease of manipulation and observation. The cryogenic methods that are employed for hydrogen are cumbersome in contrast to the laser cooling methods that are used in the early stages of our cooling technique. Furthermore, there is evidence that the collisional cross sections for evaporative cooing are more favorable for alkali atoms than for hydrogen.[29]

Evaporative cooling is accomplished by repetitively removing the high energy "tail" of the thermal distribution of atoms in the trap. The remaining atoms then cool collisionally as the high energy tail is repopulated. The essential condition for evaporative cooling is that the collision rate be sufficiently high for many collisions to occur within the lifetime of the atoms in the trap. Until now, this has not been possible using laser-cooled atoms because the atomic densities have been too low. We are confident that our dark cooling and trapping techniques provide sufficiently high densities to observe evaporative cooling.

Beside high initial density and long trapping times, evaporative cooling requires a method for selectively removing hot atoms from the trap. Our approach is to use resonant rf radiation which selectively spinflips hot atoms and thus removes

---

[26] A. Clairon, P. Laurent, A. Nadir, M. Drewsen, D. Grison, B. Lounis, and C. Salomon, "A Simple and Compact Source of Cold Atoms for Cesium Fountains and Microgravity Clocks," *Proceedings of the Sixth European Time and Frequency Forum,* Noordwijk, Netherlands, ed. J.J. Hunt, 1992.

[27] P.D. Lett, W.D. Phillips, S.L. Rolston, C.E. Tanner, R.N. Watts, and C.I. Westbrook, "Optical Molasses," *J. Opt. Soc. Am. B* 6(11): 2084-2107 (1989).

[28] N. Masuhara, J.M. Doyle, J.C. Sandberg, D. Kleppner, and T.J. Greytak, "Evaporative Cooling of Spin-Polarized Atomic Hydrogen," *Phys. Rev. Lett.* 61(8): 935-938 (1988).

[29] E. Tiesinga, A.J. Moerdijk, B.J. Verhaar, and H.T.C. Stoof, "Conditions for Bose-Einstein Condensation in Magnetically Trapped Atomic Cesium," *Phys. Rev. A* 46(3): R1167-R1170 (1992).

them from the trap.[30] The advantage of this strategy over simply lowering the magnetic trap depth is that confinement is not weakened. So far, we have tested the rf setup and shown that we can change the energy distribution function of trapped atoms with rf radiation.

2.5.4 Work in Progress

- Spin Flip Zeeman Slower

  We currently load our trap using an inverted "Zeeman slower" that has produced the largest flux of slow atoms achieved to date.[31] We have a new design that may improve the effective flux by one or two orders of magnitude by overcoming effects due to transverse heating. The key new idea is to pump the atoms from the weak field seeking hyperfine level into the strong field seeking one during the slowing process.

- Magnetic Trap with High Field Gradients

  We have designed a new magnetic trap which will produce magnetic field gradients up to 1000 G/cm, a factor of ten improvement over our current setup. Such high field gradients will be used for adiabatic compression of the trapped atoms. This will result in an increased speed of evaporative cooling.

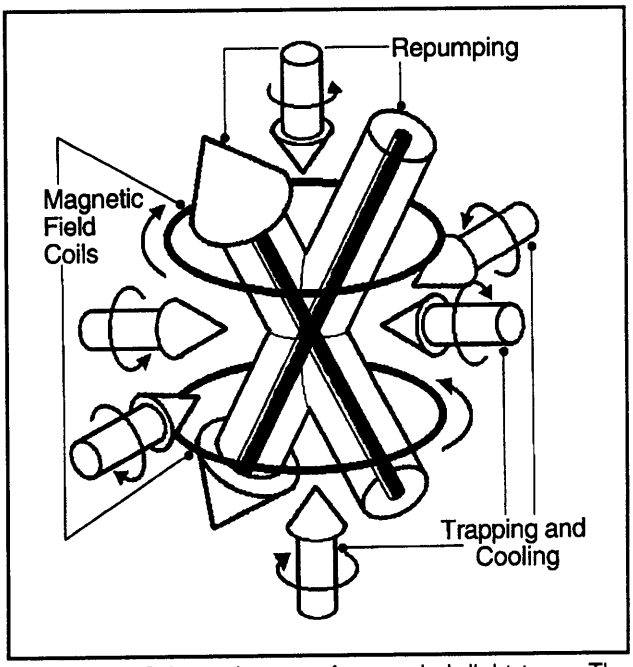

Figure 15. Schematic setup for our dark light trap. The standard light trap consists of two magnetic field coils and three orthogonal pairs of counterpropagating laser beams. In the dark light trap, two separate "repumping" beams are added which have a dark central region. This creates a small region in the center of the trap where the atoms are optically pumped into a dark hyperfine state.

2.5.5 Publications

Joffe, M.A., W. Ketterle, A. Martin, and D.E. Pritchard. "Transverse Cooling and Deflection of an Atomic Beam inside a Zeeman Slower." *J. Opt. Soc. Am. B* 10: 2257-2262 (1993).

Joffe, M.A., K.B. Davis, W. Ketterle, M.O. Mewes, D.E. Pritchard. "Experiments with Atoms Captured in a Dark Light Trap." *Bull. Am. Phys. Soc.* 38(3): 1141 (1993).

Ketterle, W., and D.E. Pritchard. Towards Higher Densities of Cold Atoms: Intense Slow Atom Beams and Dark Light Traps. *Fundamentals of Quantum Optics III, Proceedings of the Fifth Meeting on Laser Phenomena.* Lecture Notes in Physics. Ed. F. Ehlotzky. Berlin: Springer, 1993, vol. 420, pp. 77-89.

Ketterle, W., K.B. Davis, M.A. Joffe, A. Martin, and D.E. Pritchard. "High Densities of Cold Atoms in a Dark Spontaneous-force Optical Trap." *Phys. Rev. Lett.* 70: 2253-2256 (1993).

Ketterle, W., K.B. Davis, M.A. Joffe, A. Martin, and D.E. Pritchard. "Dark Spontaneous-force Optical Trap." *OSA Ann. Meet. Tech. Dig.* 16: 15-16 (1993).

Ketterle, W., K.B. Davis, M.A. Joffe, A. Martin, and D.E. Pritchard. "Kalte Natrium-Atome hoher Dichte in einer 'dunklen' Lichtdruckfalle." *Verh. DPG (VI)* 28: 417 (1993).

---

30 D.E. Pritchard, K. Helmerson, and A.G. Martin, "Atom Traps," *Proceedings of the 11th International Conference on Atomic Physics in Atomic Physics 11,* eds. S. Haroche, J.C. Gay, and G. Grynberg (Singapore: World Scientific, 1989), pp. 179-197.

31 M.A. Joffe, W. Ketterle, A. Martin, and D.E. Pritchard, "Transverse Cooling and Deflection of an Atomic Beam inside a Zeeman Slower," *J. Opt. Soc. Am. B* 10: 2257-2262 (1993).

Theses

Joffe, M.A. *Trapping and Cooling Atoms at High Densities.* Ph.D. diss., Dept. of Physics, MIT, 1993.

Pelly, J.D. *Magnetostatic Traps for Sodium Atoms.* B.S. thesis, Dept. of Physics, MIT, 1993.

2.5.6 Meeting Paper

Ketterle, W., K.B. Davis, M.A. Joffe, A. Martin, and D.E. Pritchard. "Dark Spontaneous-force Optical Trap for Sodium Atoms." Quantum Electronics and Laser Science Conference (QELS), Baltimore, Maryland, 1993, Technical Digest Series, Volume 12, p. 222.